

Simon REKERS^{1*}
Thomas AUERBACH¹
Drazen VESELOVAC¹
Fritz KLOCKE¹

CUTTING FORCE REDUCTION IN THE MILLING OF ALUMINUM ALLOYS WITH SERRATED CUTTING TOOL EDGES

Structural components for aerospace industry are in most cases milled from solid. Usually more than 80 % of the bulk material is removed by milling processes in order to obtain the parts final shape. Due to economic aspects, high material removal rates are desired to reduce cost intensive machine cycle times. In order to meet high process design demands, optimized cutting forces at maximized material removal rates are of crucial interest. These are especially depending on the work piece material to be machined, the cutter work piece engagement conditions as well as the milling cutters geometry. The usage of milling tools with serrated cutting edge geometries enables a significant reduction of cutting forces. In this article, cutting forces during milling aluminum alloys using different serration geometries and engagement conditions are investigated. At first, a generic cutting force model is introduced. The required model parameters are approximated for the machined material by subsequent milling tests employing non-serrated cutters. In a second step, a model is presented allowing a time-domain simulation to obtain cutting force variations for cutters with serrated cutting edges. Finally, experimental data for different serrated cutters are compared with the simulated predictions.

1. INTRODUCTION

The awareness of cutting force is required by machine tool designer, process analysts, tool manufacturer and process planner in order to obtain cost-efficient machining processes. Milling tools with serrated edges facilitate cutting force reduction compared to conventional milling tools whilst leaving the material removal rate unchanged. Thus higher material removal rates can be reached without causing tool breakage due to exceedance of permissible exposure limit of the tool or the tool holder.

In this paper a simulation of cutting force for milling tools with serrated cutting edges is presented similar to [3],[4],[5]. Moreover simulation results are compared to cutting force measurements. The paper is structured as follows. At first the simulation algorithm is presented. It consists of the geometrical discretization of the milling tool, a chip thickness

¹ Aachen University, Laboratory for Machine Tools and Production Engineering WZL of RWTH, Aachen, Germany

* E-mail: s.rekers@wzl.rwth-aachen.de

calculation and a subsequent calculation of the cutting force. Then the experimental test setup and the cutting force measurements are described. At last the simulation and the measurements will be compared and discussed.

2. MILLING TOOL DISCRETIZATION AND CHIP THICKNESS CALCULATION

To obtain a discretized geometry of the milling tool it is divided in N layers with a constant height b_i along the rotational axis starting from the tip of the tool. For tools with a helix angle each layer is twisted depending on the angle's value λ . The total number of layers N is dependent on the axial depth of cut a_p

$$N = \text{ceiling} \left(\frac{a_p}{b_i} \right). \quad (1)$$

In figure 1 the engagement condition for a single tool layer is depicted. Each wedge on a layer i is described by the index ij . The index j is used for a particular cutting edge. In case of a milling tool with non-serrated cutting edges and without runout each cutting edge has a constant distance to the rotational axis R_{ij} . This value can also be interpreted as local tool radius. In figure 2 the engagement condition is depicted for a milling tool with serrated cutting edges. The only difference is that the local tool radius is variable

$$R_{ij} = \begin{cases} \text{const, for non serrated cutting edges} \\ \text{var iable, for serrate cutting edges} \end{cases}. \quad (2)$$

The twist of each cutting edge can be described by the angle φ_{ij} which is the angle between the cutting edge j on layer i and a tool-fixed coordinate system.

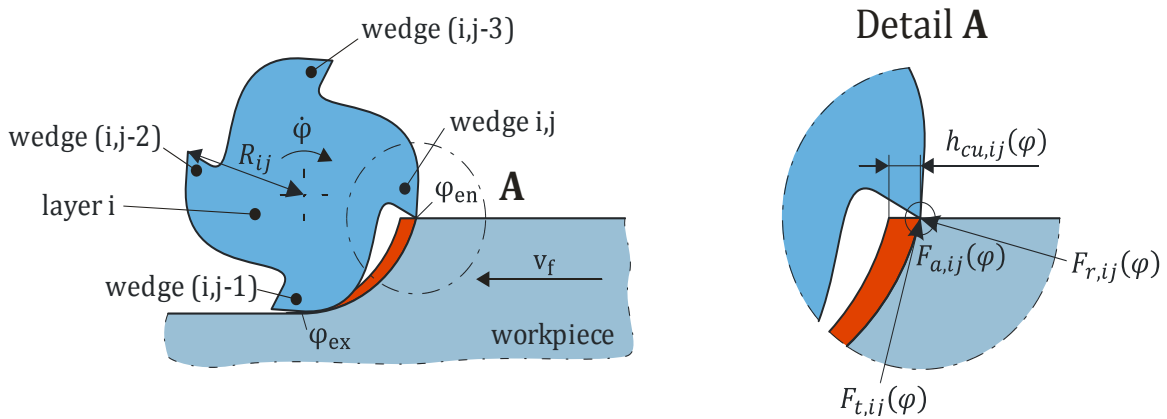


Fig. 1. Engagement of a single tool layer of a milling tool with non-serrated cutting edges

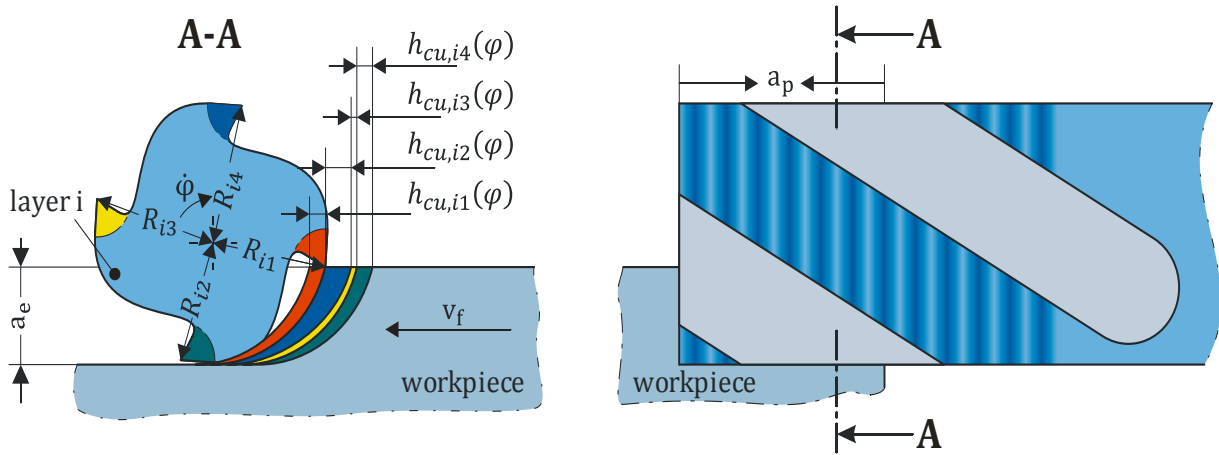


Fig 2. Engagement of a single tool layer of a milling tool with serrated cutting edges

The time dependent uncut chip thickness $h_{cu,ij}$ is obtained by modelling the milling kinematics in time-domain. The rotational axis of the milling tool is advanced in discrete time steps Δt in the direction of the feed speed v_f . Simultaneously the tool is rotated by

$$\Delta\varphi = \dot{\varphi} \cdot \Delta t. \quad (3)$$

Where $\dot{\varphi}$ is the spindle speed. With this description and the milling kinematics and a model of the workpiece the uncut chip thickness $h_{cu,ij}$ is calculated.

$$h_{cu,ij}(\varphi) = h_{ij}(90^\circ) \cdot \sin(\varphi) \cdot g(\varphi). \quad (4)$$

Where $g(\varphi)$ is a step function with the entry angle φ_{en} which is the angle when a tool enters the workpiece and φ_{ex} which is the angle when the tool leaves the workpiece. The entry angle φ_{en} and exit angle φ_{ex} are depending on the radial depth of cut a_e .

$$g(\varphi) = \begin{cases} 1, & \text{for } \varphi_{en} \leq \varphi \leq \varphi_{ex} \\ 0, & \text{else} \end{cases}. \quad (5)$$

In case of an equally pitched milling tool with non-serrated cutting edges the $h_{ij}(90^\circ)$ is equal to the feed per tooth f_z . For a milling tool with serrated cutting edges $h_{ij}(90^\circ)$ is calculated with the aid of a workpiece model. On the left side of Fig. 3 a qualitative result of the calculation of the uncut chip thickness of a milling tool with non-serrated cutting edges is shown. In this case the entry angle φ_{en} is 90 degrees and the feed per tooth f_z is 0.05 mm. The tool is equally pitched and has no runout. It can be seen that the distribution of the uncut chip thickness $h_{cu,ij}$ along a cutting edge is consistent. The maximum of $h_{cu,ij}$ is equal to the feed per tooth f_z . On the right side of Fig. 3 the distribution of the uncut chip thickness for the tool tip is depicted.

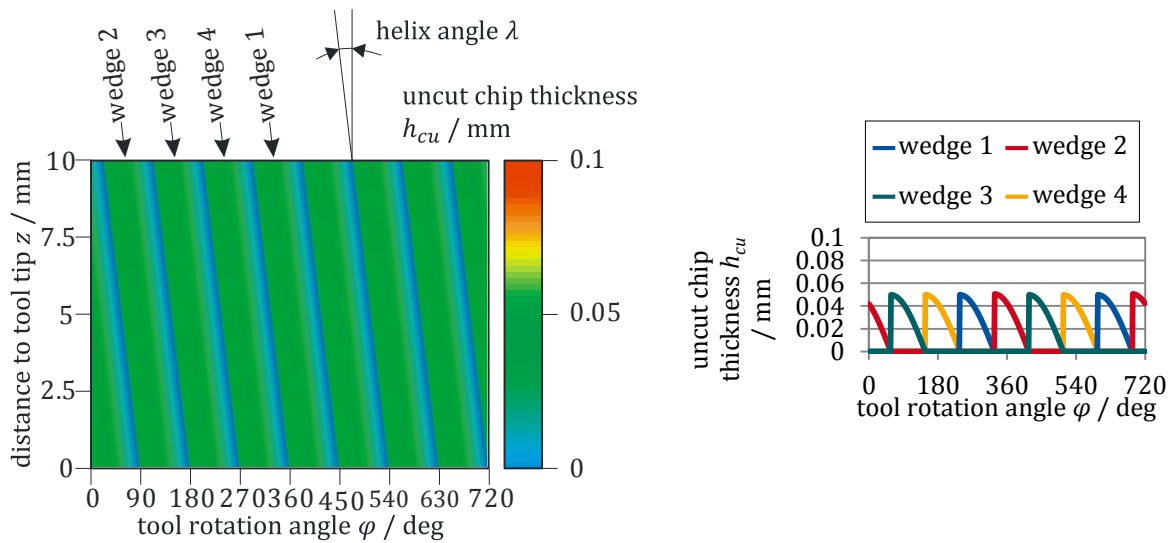


Fig. 3. Qualitative result of a uncut chip thickness for a milling tool with non-serrated cutting edges

By analogy Fig. 4 shows the distribution of the uncut chip thickness for a milling tool with serrated cutting edges for the same process parameters. Depending on the distance to the tool tip z different engagement conditions exist. On the top-right side of Fig. 4 the distribution of the uncut chip thickness for a distance to the tool-tip of 5.0 mm is shown. Only every second wedge engages the workpiece whilst the maximum chip thickness is 0.1 mm. This situation occurs when large variations in the local tool radius exist and the feed velocity is low. At a distance to the tool tip of 4.7 mm every wedge is engaging the workpiece with a variation in the maximum uncut chip thickness for each wedge.

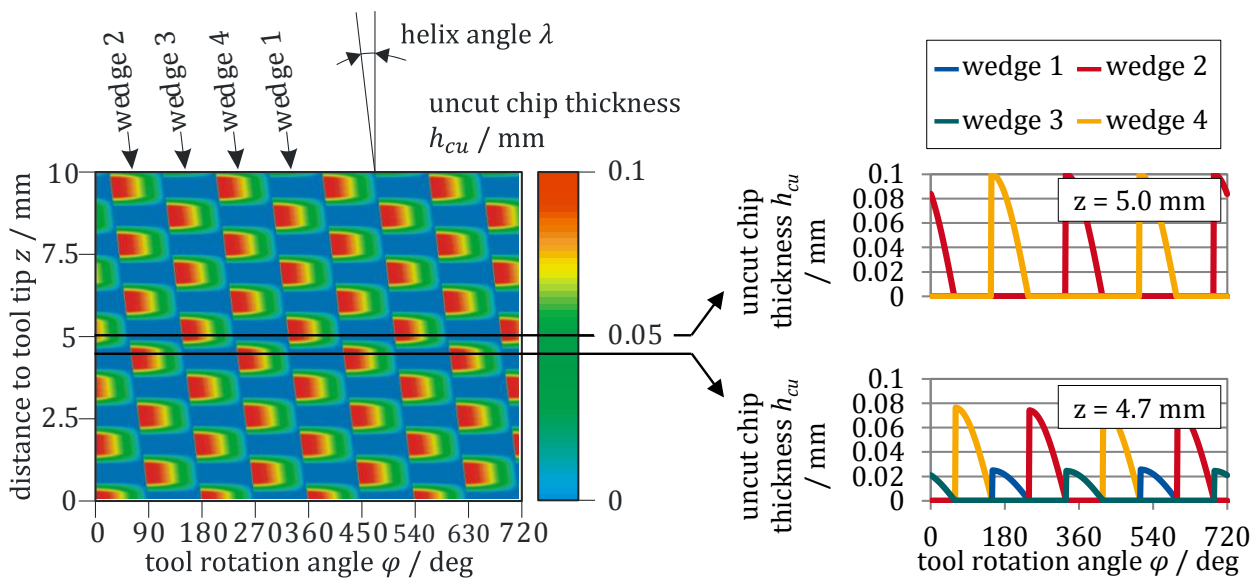


Fig. 4. Qualitative result of a uncut chip thickness for a milling tool with serrated cutting edges

3. CUTTING FORCE SIMULATION

The cutting force is predicted with the aid of a model introduced by [1]. It is a linear model which is capable of predicting cutting force for tools with an oblique, defined cutting edge geometry.

$$F = K_c \cdot b h_{cu} + K_e \cdot b. \quad (6)$$

Here h_{cu} is the uncut chip thickness, K_c a cutting coefficient and K_e a so-called edge coefficient. They depend on the workpiece material, and tool geometry. For milling tools three force components can be calculated. These are the tangential force $F_{t,ij}$, radial force $F_{r,ij}$ and axial force $F_{a,ij}$. They are depicted in Fig. 1.

$$\begin{aligned} F_{t,ij}(\varphi) &= K_{tc} \cdot b_i h_{cu,ij}(\varphi) + K_{te} \cdot b_i \\ F_{r,ij}(\varphi) &= K_{rc} \cdot b_i h_{cu,ij}(\varphi) + K_{re} \cdot b_i \cdot \\ F_{a,ij}(\varphi) &= K_{ac} \cdot b_i h_{cu,ij}(\varphi) + K_{ae} \cdot b_i \end{aligned} \quad (7)$$

The transformation equations for the cutting coefficients K_{tc} , K_{rc} and K_{ac} are given by the following equation which incorporates the friction angle β_a , the shear stress τ_s , the rake angle γ_0 and the helix angle λ .

$$\begin{aligned} K_{tc} &= \frac{\tau_s}{\sin(\varphi_c)} \frac{\sin(\beta_a - \gamma_0) \tan^2(\lambda) \sin(\beta_a)}{\sqrt{\cos^2(\varphi_c + \beta_a - \gamma_0) + \tan^2(\lambda) \sin^2(\beta_a)}} \\ K_{rc} &= \frac{\tau_s}{\sin(\varphi_c) \cos(\lambda)} \frac{\sin(\beta_s - \gamma_0)}{\sqrt{\cos^2(\varphi_c + \beta_a - \gamma_0) + \tan^2(\lambda) \sin^2(\beta_a)}}. \\ K_{ac} &= \frac{\tau_s}{\sin(\varphi_c)} \frac{\cos(\beta_a - \gamma_0) \tan(\lambda) - \tan(\lambda) \sin(\beta_a)}{\sqrt{\cos^2(\varphi_c + \beta_a - \gamma_0) + \tan^2(\lambda) \sin^2(\beta_s)}} \end{aligned} \quad (8)$$

This transformation equation is described in [1]. To transform the the force components in a workpiece coordinate system equation 9 can be applied.

$$\begin{Bmatrix} F_{ix}(\varphi) \\ F_{iy}(\varphi) \\ F_{iz}(\varphi) \end{Bmatrix} = \begin{Bmatrix} \sum_{i=1}^N \sum_{j=1}^Z -F_{tij} \cos(\varphi_{ij}) - F_{rij} \sin(\varphi_{ij}) \\ \sum_{i=1}^N \sum_{j=1}^Z F_{tij} \sin(\varphi_{ij}) - F_{rij} \cos(\varphi_{ij}) \\ \sum_{i=1}^N \sum_{j=1}^Z -F_{aij} \end{Bmatrix}. \quad (9)$$

Where N is the number of tool layers and K is the number of cutting edges on the tool.

In the following the force model is parameterized with the coefficients shown in Table 1.

Table 1. Force model coefficients used for simulation [3]

Coefficients for AL7075-T6	
β_α	$18.79 + 6.7 \cdot h_c - 0.0076 \cdot v_c + 0.2561 \cdot \gamma_0$
τ_s	$297.05 + 1.05 \cdot \gamma_0$
φ_c	$24.2 + 26.67 \cdot h_c + 0.0049 \cdot v_c + 0.3 \cdot \gamma_0$
K_{te}	$23.41 - 0.0014 \cdot v_c - 0.26 \cdot \gamma_0$
K_{re}	$35.16 - 0.0011 \cdot v_c - 0.51 \cdot \gamma_0$
K_{ae}	0

In the simulation the cutting forces for different serration geometries and process parameter are calculated. To evaluate the results characteristic values are used. At first the absolute force F is calculated by

$$F = \sqrt{F_x^2 + F_y^2 + F_z^2} . \quad (10)$$

Then the static cutting force F_{stat} , dynamic cutting force F_{dyn} , and effective cutting force F_{rms} are calculated

$$\begin{aligned} F_{stat} &= \min(F) \\ F_{dyn} &= \max(F) - \min(F) \\ F_{rms} &= \sqrt{\frac{1}{\varphi_{max} - \varphi_{min}} \int_{\varphi_{min}}^{\varphi_{max}} F^2 d\varphi} \end{aligned} . \quad (11)$$

Figure 5 shows these characteristic values in an example.

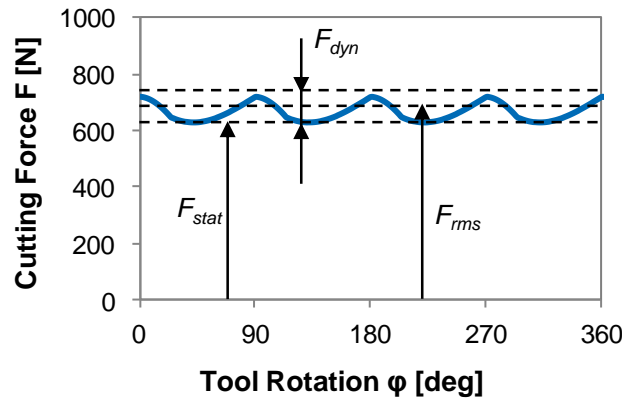


Fig. 5. Characteristic force values calculated from cutting force

In the simulation six feedrates f , four serration geometries and a non-serrated milling tool are investigated. The feedrates were stepwise increased in increments of 0.1 mm starting from 0.1 mm to 0.6 mm. As serration geometrie a Hanning window is selected which is stretched to a certain serration height s_h and a serration length s_l . In Fig. 6 the serration geometries are depicted in the top right diagramm. This geometry is helical projected onto the tool. Furthermore, the helix angle of the tool λ in the simulation is 30° . The axial depth of cut a_p is 10 mm, the radial depth of cut a_e is 5 mm an the cutting speed v_c is 70 m/min. The layer height of the disretized tool is $b_i = s_l / 20$ and the cutting force was calculated every 0.0005 s. The rake angle of the tools is $\gamma_0 = 7^\circ$. The results of the simulation are summarized in Fig. 6. They show that the effective value of the cutting force F_{rms} decreases with the cord heighth. The reduction of the effective cutting forces is greater, the stronger the serration geometry is pronounced. The lowest effective cutting forces F_{rms} exist for the simulation with a tool with the serration heitg $s_h = 0.4$ mm. Moreover it can be seen that the effective cutting force F_{rms} increases overproportional as soon as the feed per tooth f_z is higher than the serration height s_h . Beside the effective cutting force F_{rms} the static cutting

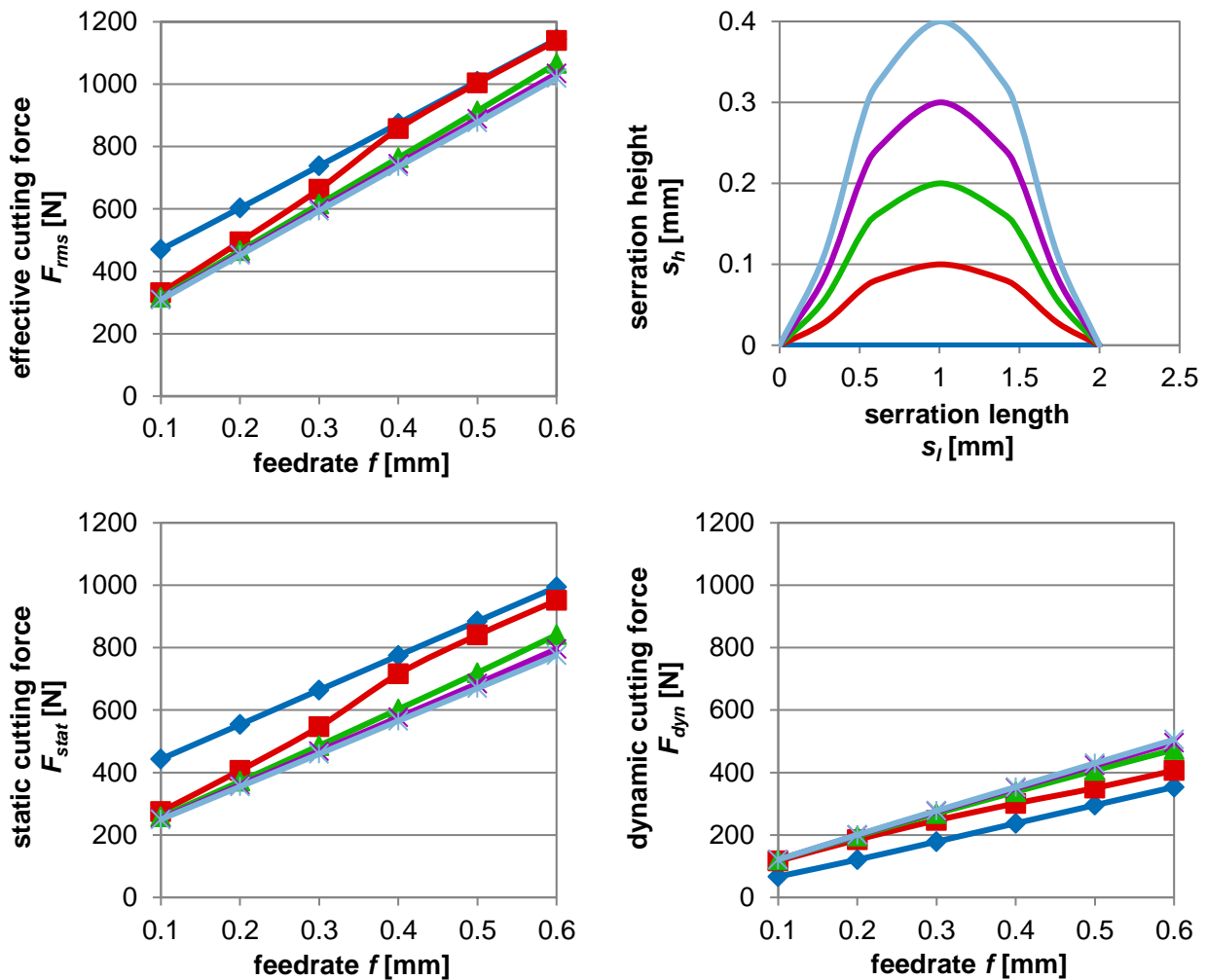


Fig. 6. Summary of the cutting force simulation

force F_{stat} decreases as well. Whilst the effective cutting force decreased 13.9% in average the static cutting force decreased by 23.3% in average. Conversely behaves the dynamic cutting force F_{dyn} . They increase by 42.8% in average compared to a tool without serrated cutting edges.

4. CUTTING FORCE MEASUREMENTS

Based on the simulation results cutting forces are measured and evaluated in analogy. In total four different tools were studied. For the force measurement a piezoelectric platform from the company Kistler is used. The type is 9255B. The force is acquired with samplerate f_s of 20 kHz and low pass filtered with a cut-off frequency of 5 khz. The cutting speed v_c is 70 m/min. The axial depth of cut is a_p is 10 mm and the radial depth of cut a_e is 5 mm. All tool parameter can be found in table 2. The serration height s_h and serration length s_l was measured on a Zoller Venturion tool measurement machine. In the trials the feed per tooth is increased stepwise starting from 0.02 mm to 0.12 mm with a stepwidth of 0.02 mm. The machined material is an aluminum alloy and the experiments were conducted on a automated test system described in [2].

Table 2. Investigated tools

No	1	2	3	4
Manufacturer	Mitsubishi Carbide			
Name	MS4SCD1000	VASFPRD1000	VAMRD1000	AMMRD1000
Diameter D	10 mm			
# Cutting edges Z	4			3
Helix angle λ	30 deg			27.5 deg
Serrated	No	Yes		
Serration height s_h	-	0.20 mm	0.32 mm	0.48 mm
Serration length s_l	-	1.00 mm	1.50 mm	2.50 mm

Figure 7 summarizes the experimental results. In the measurement it can be also seen that the effective cutting force F_{rms} decreases with the use of serration geometries. The lowest value of F_{rms} shows the tool AMMRD1000 which has the serration geometry with the highest serration height s_h and serration length s_l . The highest values of F_{rms} were observed at the tool MS4CD1000 which has no serration geometry. When the tools with four cutting edges are compared a relationship between the serration geometry and the effective cutting force can be seen. The effective cutting force always decreases with the pronunciation of the serration geometry. Also the static cutting force F_{stat} is lower for each cutting tool with serration geometry. The highest dynamic cutting F_{dyn} is present for the tool with the highest serration length s_l and serration height s_h . Other than in the simulation the second highest dynamic cutting force F_{dyn} was measured for the tool without serration

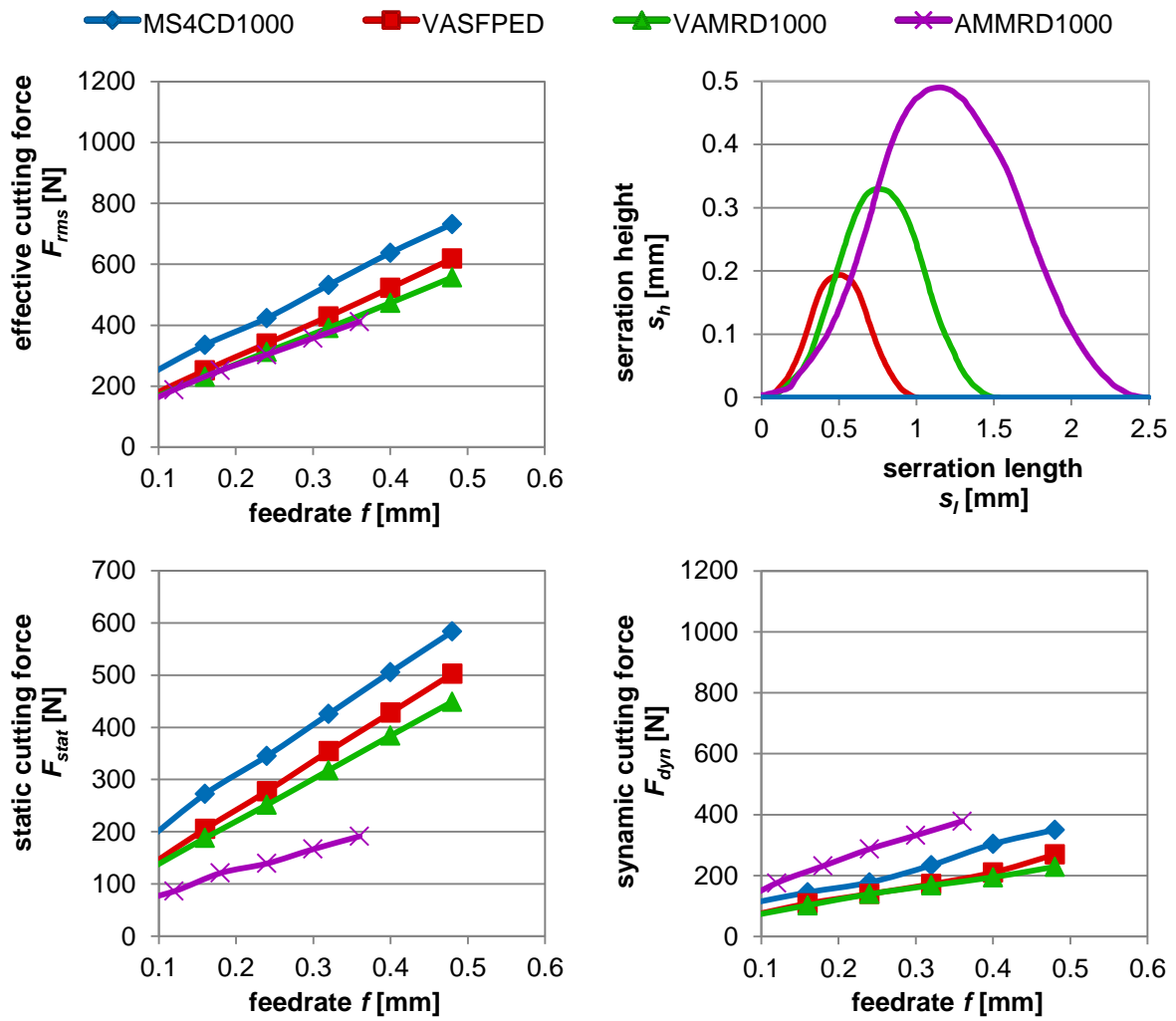


Fig. 7. Summary of the cutting force measurement



Fig. 8. Investigated tools and chips

geometry. In Fig. 8 the generated chips are depicted together with a picture of the investigated tools. All tools with serration geometries generate small, easy to evacuate chips.

The simulation and the measurement show a qualitative good correlation. Differences in the quantity of the force values can be apparent. A possible reason is that the applied force model does not fit to the machined material. However, both simulation and measurement confirm that milling tools with serrated cutting tool edges provide a possibility to reduce cutting force whilst maintaining the same material removal rate.

5. CONCLUSION

In this article a cutting force simulation for milling tools with serrated cutting edges is presented. At first an approach for the calculation of a chip thickness distribution is introduced. Then, with the aid of common force model, the cutting force is calculated. The presented simulation is compared to real cutting test. In the results a good qualitative correlation between the results can be seen. Both in the simulation and in the measurement the static cutting force and the effective cutting force are lower for cutting tools with serrated cutting edges. Thereby milling tools with serrated cutting edges provide a good solution to decrease the cutting force whilst maintaining the productivity.

ACKNOWLEDGMENTS

The authors would like to thank the German Research Foundation DFG for the support of the depicted research within the Cluster of Excellence "Integrative Production Technology for High-Wage Countries".

REFERENCES

- [1] ALTINAS Y., 2000, *Manufacturing Automation: Metal Cutting Mechanics, Machine Tool Vibrations and CNC Design*, Cambridge.
- [2] AUERBACH T., REKERS, S., VESELOVAC D., KLOCKE F., 2013, *Determination of characteristic values for milling operations using an automated test and evaluation system.*, Advanced Manufacturing Engineering and Technologies NEWTECH, Stockholm, Sweden.
- [3] DOMBOVARI, Z., ALTINAS, Y., 2000, *The Effect of Serration on Mechanics and stability of milling cutters*, International Journal of Machine Tools and Manufacture, 50/6, 511-520.
- [4] FERRY, W., 2008, *Virtual Five-Axis Flank Milling of Jet Engines Impeller*, University of British Columbia.
- [5] MERDOL D., ALTINAS Y., *Mechanics and Dynamics of Serrated Cylindrical and Tapered End Mills*, Journal of Manufacturing Science and Engineering, 126/2, 317-326.